이학석사 학위논문

Downward influences of Sudden Stratospheric Warming (SSW): 2018 SSW nudging experiment

2018 성층권 돌연승온 너징 실험에서 모의된 성층권-대류권 연직 접합

2023년 2월

서울대학교 대학원

지구환경과학부

홍 동 찬

Downward influences of Sudden Stratospheric Warming (SSW): 2018 SSW nudging experiment

2018 성층권 돌연승온 너징 실험에서 모의된 성층권-대류권 연직 접합

지도교수 손 석 우

이 논문을 이학석사 학위논문으로 제출함
2022년 10월

서울대학교 대학원
지구환경과학부
홍 동 찬

홍동찬의 이학석사 학위논문을 인준함
2023년 1월

위 원 장 최 우 갑 (인)
부위원장 손 석 우 (인)
위 원 박 성 수 (인)

Abstract

The downward influences of 2018 Sudden stratospheric warming (SSW) are examined by nudging the zonal-mean stratospheric state above 90-hPa in the global climate model, Global/Regional Integrated Model system (GRIMs). The free-running experiment (FREE) fails to forecast the SSW because of the long lead time, 18 days before the onset. However, the nudged experiment (NUDGED) simulates the positive polar-cap averaged geopotential height anomaly index (PCI) in the troposphere and the negative phase of the North Atlantic Oscillation (NAO) compared to FREE. The geopotential and surface pressure budget analyses are performed to examine a mechanism for the downward influences. When PCI differences are decomposed to the surface and thickness portions, an increase of surface pressure near the SSW onset explains the tropospheric PCI differences. The surface pressure budget shows strong mass convergence above 50-hPa near the SSW onset in NUDGED, contributing to the increase in surface pressure. Nudged easterly induces poleward circulation in the polar stratosphere, and this dynamic process is verified by two sensitivity tests. This result indicates that although there is less air mass in the stratosphere, an anomalous event like SSW can contribute to the change in the surface pressure and suggest a new possible mechanism for the downward influences of SSWs.

Keywords: SSW, Nudging, Downward influence, PCI, Mass convergence.

Student Number: 2021-29047

Table of Contents

List of tables

List of figures

experiments. The evolution of polar-cap averaged surface pressure budgets for each vertical range in (d) NUDGED, (e) FREE, and (f) differences. The dashed black lines indicate the onset date of the SSW. The lower panels' light gray, green, and blue lines indicate the surface pressure budgets from the whole vertical layers, troposphere, and stratosphere. Dotted areas and solid marked lines indicate statistical significance at the 95% confidence level according to a Student's t-test.

Fig. 6. Time-pressure development of the polar-cap (65-90° N) averaged differences between two experiments (NUDGED-FREE) in (a) zonal wind, (b) meridional wind, (c) convergence, and (d) vertical wind. The dashed black lines indicate the onset date of the SSW, and the green lines indicate the 90-hPa pressure level. Dotted areas indicate statistical significance at the 95% confidence level according to a Student's t-test.

Fig. 7. Time-pressure development of the polar-cap (65-90° N) averaged differences between two experiments (NUDGED-FREE) performed by GloSea6 in (a) zonal wind, (b) air temperature, (c) meridional wind, and (d) geopotential height. The dashed black lines indicate the onset date of the SSW, and the green lines indicate the 90-hPa pressure level. Dotted areas indicate statistical significance at the 95% confidence level according to a Student's t-test.

Fig. 8. Same as Fig. 7, but for the differences between FREE and T-NUDGED, only-temperature nudging experiment performed by GRIMs.

Fig. 9. The schematic diagram of the dynamic process in the SSW nudging experiment.

Fig. 10. Same as Fig. 4, but for the polar-cap (65-90° N) averaged geopotential height anomalies during 40 SSWs defined by Charlton and Polvani (2007) in JRA-55.

1. Introduction

A climatological strong and cold westerly named polar vortex exists in the wintertime polar stratosphere. However, the polar vortex sometimes breaks down because of the planetary scale of waves propagating upward from the troposphere. Then there is a rapid temperature increase in the polar stratosphere accompanied by a reversal of westerly to easterly. This event occurs in just a few days and is named Stratospheric Sudden Warming (SSW). Because of its rapid changes, the SSWs are the most dramatic events in the polar stratosphere during wintertime.

Although the SSWs are phenomena in the stratosphere, their effects are not limited to the stratosphere. After SSWs, negative Northern Annular Mode (NAM) in the stratosphere descends to the troposphere on average (Baldwin et al., 2003). The negative NAM lasts about two months in the troposphere longer than in the stratosphere because of the faster radiative timescale (Baldwin et al., 2021). Also, the equatorward shift of the storm track in the troposphere is observed during a weak polar vortex, and the poleward shift is also observed during a strong polar vortex (Baldwin and Dunkerton, 2001). The downward influences of SSWs

are also observed on the surface (Butler et al., 2017; Domeisen and Butler, 2020). In the composites of the historical SSWs, there are anomalous high sea level pressure anomalies (SLP) near the North pole and low SLP anomalies in the mid-latitudes. Also, there are cold anomalies in Northern Eurasia and warm anomalies in the northeast region of North America. Consistent with the equatorward shift of the storm track, precipitation in southern Europe increases but decreases in northern Europe. Because of the effects above, there are more surface extremes, like cold air outbreaks and floods, projected well onto the negative phase of the North Atlantic Oscillation (NAO) (Domeisen et al., 2020). Also, Song et al. (2015) investigates the effects of SSWs in East Asia and shows the cold surface air temperature anomalies during extreme SSW events.

The S2S timescale indicates a time range of about 10 to 30 days, so the atmosphere is influenced by both the initial and boundary conditions (White et al., 2017). These conditions have different temporal and spatial scales, so the forecasts in the S2S timescale are challenging now. Also, because of these long-lasting impacts of SSWs on the surface, SSWs have been studied actively as forecast factors in the sub-seasonal to seasonal (S2S) timescale (Karpechko et al., 2018; Rao et al., 2020; Sigmond et al., 2013).

Tripathi et al. (2015) and Domeisen et al. (2020b) say that there are differences in the prediction skill of the surface after 2–4 weeks from the initialization according to the stratospheric state. When the stratospheric conditions in initial states show a strong or weak polar vortex, the forecasts show higher forecast skill than the normal polar vortex.

However, all SSWs do not show downward influences on the troposphere and surface (Nakagawa and Yamazaki, 2006). Several studies suggest factors, the dominant wavenumber of the preceding upward wave flux (Nakagawa and Yamazaki, 2006), the displacement/split type of SSWs (Huang et al., 2018; Mitchell et al., 2013; Seviour et al., 2013), the strength of polar vortex during SSWs (Rao et al., 2020), to determine whether the negative NAM after SSWs propagate downward to the troposphere. Although there are so many previous studies, which factor is the most important is still being determined. Also, the S2S models can not forecast SSWs very well, and fewer than 50% of ensemble members predict the SSW at lead times of two weeks (Domeisen et al., 2020a). There is case variability in predicting the SSW. Rao et al. (2019) find that the predictability of the 2019 January SSW is longer than two weeks in the Beijing Climate Center Forecast System (BCC_CSM).

However, the deterministic predictable limit of the 2018 February SSW is 1–2 weeks in the same forecast system because the precursors of the 2018 February SSW are hard to forecast (Rao et al., 2018). Although the importance of SSWs is introduced well now, their influences are hard to study because of their poor predictability and uncertain downward influences.

Also, the mechanisms for the downward influences of SSWs still need to be fully understood. Several studies like the remote effects of wave driving in the stratosphere (Thompson et al., 2006), planetary wave absorption and reflection (Kodera et al., 2016), direct effects on baroclinicity (Smy and Scott, 2009), and remote effects of stratospheric potential vorticity anomalies (Black, 2002) are suggested to address the downward influences. These studies explain the influences using the momentum changes after SSWs and their projection onto the surface. However, these studies could not explain the surface amplification, indicating that the pressure anomalies on the surface are higher than those in the stratosphere. A new mechanism is necessary to explain the influences of SSWs and surface amplification.

In this study, nudging is used for simulating the perfect SSW during model integrations to investigate the downward influences of

SSWs in this study. First, nudging is conducted by relaxing the model's state to the time-evolving observation state only in the stratosphere. Next, the downward influences of SSWs are investigated by differentiating the troposphere and surface of free-evolving and nudged experiments. Afterward, geopotential and surface pressure budget analysis is performed to explain the influences from stratospheric nudging. Finally, the mechanism is suggested by comparing the stratospheric circulation in each experiment and verified by other sensitivity tests.

2. Data and Methods

2.1. Reference datasets

The fifth-generation European Centre for Medium-range Weather Forecasts atmospheric reanalysis (ERA5; Hersbach et al., 2020) and the Global Precipitation Climatology Project (GPCP; Adler et al., 2016) are used for reference datasets in this study. All variables have the same temporal (daily) and horizontal resolution (1.5° × 1.5°). Air temperature (T), zonal wind (U), surface air temperature (SAT), sea level pressure (SLP), and geopotential height (Z) are obtained from the ERA5 dataset. The anomalies from ERA5 are defined as deviations from the daily climatology from 1979 to 2018 (40 years). However, the climatology of precipitation (Pr), obtained from GPCP, has a different period (1997-2021) because of its temporal coverage.

2.2. Description of GRIMs model

The Global/Regional Integrated Model system (GRIMs), which has been updated to version 4.0 recently, is used for numerical experiments in this study. The physics schemes of

GRIMs are updated to state-of-the-art physics schemes in Weather Research and Forecasting (WRF) version 4.0. The details of the model configuration are described in Table 1. The model resolution is set to T126L64 with a hybrid-sigma vertical coordinate. T126L64 designates that the truncated total wavenumber is 126 with 64 vertical layers (upper boundary at 0.3 hPa). The model is integrated for 45 days, starting 18 days before the 2018 SSW onset date (lag -18 days). Five atmospheric variables are needed for initial conditions: three-dimensional geopotential height, zonal wind, meridional wind, air temperature, and specific humidity. Sea surface temperature (SST) and sea ice concentration (SIC) are prescribed and updated daily for boundary conditions. The atmospheric and boundary variables are taken from the ERA5 dataset with a 0.25° × 0.25° and Daily Optimum Interpolation Sea Surface Temperature (DOISST; Huang et al., 2021) version 2.1 with a 0.125° × 0.125° horizontal resolution, respectively.

2.3. Nudging experiment designs

The nudging is the method that makes the state of the model relaxed to the reference state, and its equation is expressed as

$$\frac{\partial X}{\partial t} = -\frac{X - X_r}{\tau}, \quad (1)$$

where τ is the nudging timescale, which indicates the strength of nudging. X, X_r, $\mathrm{F(X)}$, and $\frac{\partial X}{\partial t}$ are the state of the model, reference state (observation in this study), the tendency of $\mathbf{X}$ calculated from the model, and the updated tendency of $\mathbf{X}$ after combining the nudging effect. Eq. (1) is applied at every time step during integration to reduce the model's bias. In this study, the nudging method in the Stratospheric Nudging and Predictable Surface Impacts (SNAPSI; Hitchcock et al., 2022) project, which aims to evaluate the impacts of SSW on the tropospheric prediction from a multi-model perspective, is used. The ERA5 is used as a reference state, so six hourly zonal wind and air temperature in the ERA5 dataset are used for nudging. The only zonal-mean components of variables in the stratosphere (over 90-hPa) are nudged to the reference state, and the nudging timescale is set to six hours, so the model's state is almost the same as the reference. There are two experiments, FREE and NUDGED (Table. 2). FREE is a free-running experiment, and NUDGED is an experiment nudged to reference state by using the above method.

The 2018 boreal major SSW event (hereafter 2018 SSW) is used in this study. The onset date of 2018 SSW was 12 Feb 2018,

and 2018 SSW is categorized to split type (split−displacement type in Choi et al., 2019). After the 2018 SSW, there were negative phases of NAM and NAO in the troposphere, consistent with the averaged responses after SSWs. Also, there was cold weather over North Eurasia for the last two weeks of Feb, so this case is selected for study because of its clear downward impacts.

2.3. Geopotential & Surface pressure diagnostics

The geopotential budget equation expressed below is used to investigate reasons for polar−cap geopotential height anomaly index (PCI) differences between FREE and NUDGED.

$$\frac{\partial \Phi}{\partial t} = \left(\frac{R_d \cdot T_s}{p_s}\right)\frac{\partial p_s}{\partial t} + \int_{p_s}^{p} -\frac{R_d}{p'}\frac{\partial T_v}{\partial t}\,dp', \quad (2)$$

Φ, T, T_v, and p are the geopotential, air temperature, virtual temperature, and pressure. The R_d indicates the dry air gas constant, and the subscript s refers to the surface. The geopotential at a specific pressure level is modulated by the change of surface pressure and vertical integration of temperature below the pressure level so that we can call the first term of RHS a surface term and the second term of RHS a thickness term. Because the surface term is independent of any pressure levels, the whole vertical geopotential increase when the surface pressure increases.

However, the increase in air temperature can modulate only above geopotential. All variables used to calculate the geopotential budget have the same temporal (six hourly), horizontal (1.5° × 1.5°), and vertical (34 pressure levels) resolution.

the surface pressure budget equation is performed by two model experiments, to explain a change of surface pressure in Eq. (2).

$$\frac{\partial p_s}{\partial t} = \int_{p_s}^{0} -\nabla \cdot (\vec{u}\,\Delta p')\, dp', \quad (3)$$

$\vec{u}$ and $\Delta p'$ mean the horizontal wind vector and the vertical pressure differences in model-level resolution. RHS means the vertical sum of mass flux convergence above a grid, so surface pressure increases as the mass converges. By Eq. (3), we can quantify the contribution of mass flux convergence at each level. Unlike in the geopotential budget equation, all variables used to calculate the surface pressure budget are in the model's native resolution for accurate budgets.

3. Results

3.1. Downward influences of nudged 2018 SSW

The zonal-mean zonal wind at 10-hPa and 60° N and polar-cap (65-90° N) averaged air temperature at 10-hPa are shown in Figure 1 to compare the predictability of 2018 SSW in FREE and NUDGED. The NUDGED simulates the wind reversal of westerly to easterly and the sudden increase of air temperature up to about 240 K successfully. However, the FREE fails to predict 2018 SSW and simulates a strong polar vortex in the stratosphere because of the long lead time, initiated 18 days before the SSW onset. All ensemble members in FREE do not simulate any wind reversal and show very cold air temperatures in the polar stratosphere. Other S2S models initiated 18 days before the onset also failed to forecast 2018 SSW (Karpechko et al., 2018). To check the predictability for SSW in GRIMs, no perturbed one member of FREE initiated on 2nd Feb 2018, 10 days before the SSW onset. The experiment succeeded in simulating the wind reversal and air temperature increase (not shown). So GRIMs model shows similar performance for forecasting SSW to other numerical models.

The PCI in ERA5 and two experiments are shown in Figure 2

to check the downward influences of the stratosphere. In ERA5, the PCI shows a positive value in the stratosphere at SSW onset, and its influence is also shown in the troposphere (Figure 2a). The increase in air temperature at the polar stratosphere makes such positive PCI in the stratosphere. However, the FREE simulates negative PCI in the polar stratosphere because of cold air temperature (Figure 2b). Also, the development of PCI in FREE is different from that in ERA5. The NUDGED simulates the positive PCI in both spheres and the statistically significant positive PCI difference (NUDGED−FREE) in the troposphere (Figure 2d). Also, there is surface amplification about ten days after the SSW onset. The same two experiments, initiated on 8th Feb 2018, are performed to check the performance for simulating downward influences in the GRIMs model. Then the FREE and NUDGED show almost the same PCI in the troposphere up to 1st Mar, so the downward influences in the GRIMs model are dependent on the initiation dates.

The surface air temperature, sea−level pressure, and precipitation anomalies averaged for 20 days from SSW onset are shown in Figure 3 for stratospheric surface effects. In observation, there are cold anomalies in northern Eurasia and warm anomalies in

North America and the North pole (Figure 3a). However, the warm anomalies in the north pole exist before the SSW, so they are not effects of the 2018 SSW. There are high-pressure anomalies at the North pole and low-pressure anomalies at the low latitude. However, the anomalous high in the north-eastern pacific seems to be the teleconnection pattern of La Nina (Figure 3b). The precipitation anomalies in GPCP also show more precipitation in western Europe (Figure 3c). So the observation data show the partial patterns of a negative phase of NAO, which are traditionally after SSWs. When comparing the FREE and NUDGED, NUDGED simulates significant cold anomalies in northern Eurasia and warm anomalies in northern North America (Figure 3d). Also, the dipole pattern (anomalous high at the North pole and anomalous low in Europe) is shown in the sea-level pressure differences. The precipitation differences show more precipitation in western Europe because of the equatorward of the storm track. So NUDGED simulates the averaged responses of SSWs compared to FREE. The differences between FREE and NUDGED are different from the observed anomalies. Because differences between the two experiments only come from the differences in the stratospheric state, but the observations' anomalies are results of the

stratosphere and other phenomena like global warming and La Nina.

It is verified that only-stratospheric state nudging can influence the troposphere and surface by the simulated positive PCI and negative NAO. Moreover, the surface effects after SSW are related to the positive PCI, so it is essential to investigate the reason for positive PCI differences.

3.2. Budget analyses for PCI differences

To check each contribution of surface and thickness, we decompose the PCI differences between the two experiments into the surface (at 1000-hPa) and thickness (differences from 1000-hPa) portions (Figure 4 upper row). The PCI differences in the surface portion (Figure 4b) show statistically significant positive values in the troposphere and explain whole tropospheric PCI differences in Figure 4a. Unlike the surface portion, there are tropospheric negative PCI differences in the thickness portion about ten days after SSW onset (Figure 4c), and they induce the surface amplification mentioned in Figure 2d. However, the PCI differences in the stratosphere are explained by the thickness portion, so each term's contribution to PCI differences depends on the vertical level.

Such an increase in surface geopotential is related to the

increase in surface pressure. So the geopotential height budgets are also decomposed to the surface and thickness portions (Figure 4 lower row). First, there is a strong and long geopotential increase over the 300-hPa near the SSW onset, and this makes the positive and long-lasting PCI in the stratosphere (Figure 4f). Also, there is a substantial increase in surface geopotential near the SSW onset (Figure 4e), which induces long-lasting PCI differences in the troposphere. This geopotential increase in the surface is the result of the increase in surface pressure at the North pole, and this surface pressure increase is consistent with the previous surface effects (sea-level pressure anomalies). The surface pressure increases after SSWs are commonly observed after SSWs. However, the reason for the surface pressure increase has yet to be fully explained by the previous studies so far.

So the surface pressure budget analysis is performed by two experiments to explain the surface pressure evolution. Eq. (3) calculates the convergence of mass flux in each vertical level and shows each level's contribution to the surface pressure increase. The surface pressure budgets and differences between the two experiments are shown in Figure 5. When comparing the FREE and NUDGED, the two experiments show similarities up to about 10

days (Figure 5a, b). However, there are a few differences in the stratosphere near the SSW onset, NUDGED simulates the substantial mass convergence above 60 hPa (Figure 5b). Also, there are mass divergences in the lower troposphere and convergences near the tropopause in NUDGED. However, FREE does not simulate any features shown in NUDGED (Figure 5a). So above features stand out in the differences between the two experiments (Figure 5c).

We divide the whole vertical level by 150-hPa to quantify the contribution of the troposphere and stratosphere. Strictly speaking, 150-hPa is in the stratosphere but selected to exclude the mass convergence near the tropopause after SSW onset. As a result, the surface pressure tendency from all vertical layers in NUDGED recovers rapidly near the SSW onset because of the mass convergence in the stratosphere (Figure 5d). However, FREE does not simulate such recovery in surface pressure tendency, and there are substantial differences in the contribution of the stratosphere with NUDGED (Figure 5e). In differences between the two experiments, the stratosphere increases the surface pressure, but the troposphere plays the opposite role (Figure 5f). The mass convergences above 60-hPa in Figure 5c induce such

stratosphere's contribution. Also, these surface pressure budgets verify that the previous insignificant surface geopotential increase is due to the cancel-out by mass divergence in the troposphere.

The geopotential budgets verify that the positive PCI differences between NUDGED and FREE in the troposphere come from the surface. Moreover, the surface pressure budgets show that this geopotential increase in the surface results from mass flux convergence in the stratosphere near the SSW onset. This mass convergence seems to result from artificial nudging because there are drastic changes along 60-hPa. So we should investigate the dynamic process of how nudging changes the circulation in the stratosphere. Also, there are statistically significant strong mass convergences near the tropopause and divergences in the lower troposphere after the SSW onset, but we want to focus on mass convergence in the stratosphere in this analysis.

3.3. Circulation changes by nudged SSW

The evolutions of polar-cap averaged zonal wind, meridional wind, convergence, and vertical wind differences (NUDGED-FREE) are shown in Figure 6. First, the differences in zonal wind show significant easterly anomalies in the stratosphere and troposphere

because of nudging (Figure 6a). There are also differences in the meridional wind despite no nudging. The meridional wind differences are statistically significant positive above 60-hPa, but negative below 60-hPa (Figure 6b). In the troposphere, there are negative differences near the surface but positive differences near the tropopause after the SSW onset. These differences in the meridional wind are related to the differences in convergence. Because the convergence means the meridional wind at a specific latitude when averaged over the polar-cap region. Although the polar-cap averaged convergence and meridional wind are not the same, the two variables show very similar time evolution patterns. So the differences of polar-cap averaged convergence show positive values in the stratosphere (Figure 6c), and we can check that the meridional wind determines the convergence/divergence at the North pole. When comparing the mass flux convergence in Figure 5, the convergences in Figure 6c are not multiplied by the mass in each level, so it shows high values in the upper stratosphere. Moreover, these convergences induce the downward vertical wind at the North pole in both the stratosphere and troposphere. We can hypothesize that the nudged easterlies change the meridional wind poleward by acting as a positive Coriolis force,

and this poleward circulation makes mass flux convergence and downward motion at the North pole. This hypothesis is not based on the quantitative results of momentum budgets but on the qualitative interpretation of four variables. So this should be justified by other sensitivity tests.

The same FREE and NUDGED experiments are performed by an operational model, Global Seasonal forecasting system version 6 (GloSea6; Kim et al., 2021), used in Korea Meteorological Administration (KMA) to check inter-model sensitivity. The differences between the two experiments of polar-cap averaged zonal wind, air temperature, meridional wind, and geopotential height are shown in Figure 7. NUDGED, performed by GloSea6, simulates easterly anomalies and positive meridional wind anomalies in the stratosphere compared to FREE (Figure 7a, c). The PCI differences also show positive values in the stratosphere and troposphere, like those performed by GRIMs (Figure 7d). The stratospheric PCI differences come from the nudged warm temperature anomalies (Figure 7b). However, the tropospheric PCI differences come from the surface (not shown). So GloSea6 simulates the same meridional circulation changes induced by nudging with those in GRIMs. It is verified that the downward

influences of nudged SSW are independent of the numerical model.

The additional nudging experiment, the only-temperature nudging experiment (T-NUDGED), is performed by the GRIMs model to check the sensitivity of the nudging method. The differences between FREE and T-NUDGED of the same variables in Figure 7 are shown in Figure 8. In this experiment, we do not apply nudging to the zonal wind. However, the thermodynamic circulation by nudged warm temperature anomalies induces easterly anomalies (Figure 8a, b). The differences in easterly anomalies between NUDGED and T-NUDGED are only the timings when the easterly anomalies occur. T-NUDGED shows easterly anomalies later than NUDGED. And because of these differences, there are negative meridional wind differences near the SSW onset but positive differences after the negative anomalies (Figure 8c). These equatorward winds induce mass divergence in the stratosphere, so there are negative PCI differences in the troposphere near the SSW onset (Figure 8d). As the meridional wind differences change from negative to positive, the PCI differences in the troposphere also change to positive. So it is verified that the meridional wind in the stratosphere can affect the PCI in the troposphere by mass flux.

The changes in the stratospheric circulation in GRIMs indicate the dynamic process that the nudged easterly anomalies induce the poleward circulation and mass flux convergence at the North pole in the stratosphere. This process is also shown in GloSea6 nudging experiments, so it is not sensitive to the model. However, the response timing is shifted later when the nudging method is changed to nudging temperature only. So we conclude that only the zonal-mean stratospheric state induced by 2018 SSW can influence the troposphere and surface by modulating the meridional circulations in the numerical model.

4. Conclusions and Discussion

This study investigates the downward influences of 2018 SSW and its mechanism by nudging the zonal-mean stratospheric state into the numerical model. NUDGED, which simulates SSW, simulates the positive PCI differences in the troposphere and surface amplification compared to FREE, which fails to predict SSW. Also, the differences between the two experiments in surface variables show that NUDGED simulates the negative phase of NAO compared to FREE. So we can conclude that the numerical model can qualitatively simulate the averaged influences of SSWs when the only stratosphere is nudged to SSW. Then budget analyses are performed to explain the positive PCI differences shown in NUDGED and FREE. The PCI differences in the troposphere come from the surface term not from the thickness term. And the surface pressure increase near the SSW onset induces such geopotential increase in the surface. This surface pressure increase results from strong mass flux convergence in the stratosphere, modulated by the nudged easterly anomalies. And these circulation changes are not sensitive to numerical models but sensitive to the nudging variables. These above dynamic processes are illustrated in Figure 9. In

climatology, there is strong westerly in the winter polar stratosphere. But when SSW occurs (in this case, nudged SSW), the westerly reverses to the easterly, and this easterly acts as the poleward Coriolis force (Figure 9 left). The poleward air motion makes the mass convergence in the stratosphere, and this mass convergence shows an instantaneous and barotropic response to the surface (Figure 9 right). So this circulation change after SSW increases the surface pressure, and although there is less air mass in the stratosphere, an anomalous event like SSW can contribute to the change in the surface pressure.

The reason for PCI differences near the SSW onset is investigated in this study, but the later processes are not considered now. In observation, there is the biggest anomaly about 40 days after the SSW onset, and the geopotential increase near the SSW onset can not explain this. So the following study should explain these processes. Moreover, the suggested dynamic process in this study can not guarantee the downward influences in observation or reanalysis data. However, when the methods in this study are applied to 40 SSWs defined by CP07 in Japanese 55-year Reanalysis (JRA-55; Kobayashi et al., 2015), the tropospheric PCI comes from the surface (Figure 10b). Also, the significant

geopotential increases near SSW onset are verified by geopotential budget analysis (Figure 10e). We will try to explain the whole and general processes during SSWs through additional analyses in reanalysis data. So this study is significant in the sense that it suggests a new methodology and possible mechanism for the downward influences of SSWs.

References

Adler, R. F., and Coauthors, 2018: The Global Precipitation Climatology Project (GPCP) monthly analysis (New Version 2.3) and a review of 2017 global precipitation. *Atmosphere*, **9**(4), 138

Baldwin, M. P., Stephenson, D. B., Thompson, D. W., Dunkerton, T. J., Charlton, A. J., and O' Neil, A., 2003: Stratospheric memory and skill of extended-range weather forecasts. *Science*, **301**(5633), 636-640

Baldwin, M. P., and Coauthors, 2021: Sudden stratospheric warmings. *Reviews of Geophysics*, **59**(1), e2020RG000708.

Baldwin, M. P., and Dunkerton, T. J., 2001: Stratospheric harbingers of anomalous weather regimes. *Science*, **294**(5542), 581-584

Black, R. X., 2002: Stratospheric forcing of surface climate in the arctic oscillation. *Journal of Climate*, **15**(3), 268-277

Butler A. H., Sjoberg, J. P., Seidel, D. J., and Rosenlof, K. H., 2017: A sudden stratospheric warming compendium. *Earth Syst. Sci. Data*, **9**(1), 63-76

Charlton, A. J., and Polvani, L. M., 2007: A new look at stratospheric sudden warmings. Part 1: Climatology and modeling benchmarks. *J. Climate*, **20**(3), 449–469

Choi, H., Kim, B.-M., and Choi, W. 2019: Type classification of Sudden Stratospheric Warming based on Pre- and Postwarming periods. *Journal of Climate*, **32**(8), 2349–2367

Domeisen, D. I. V., and Coauthors, 2020a: The role of the stratosphere in subseasonal to seasonal prediction: 1. Predictability of the stratosphere. *Journal of Geophysical Research: Atmospheres*, **125**(2), e2019JD030920

Domeisen, D. I. V., and Coauthors, 2020b: The Role of the Stratosphere in Subseasonal to Seasonal Prediction: 2. Predictability Arising From Stratosphere–Troposphere Coupling. *Journal of Geophysical Research: Atmospheres*, **125**(2)

Domeisen, D. I. V., and Butler, A. H., 2020: Stratospheric drivers of extreme events at the Earth's surface. *Commun. Earth Environ.*, **1**, 59

Domeisen, D. I. V., Grams, C. M., and Papritz, L., 2020: The role of North Atlantic–European weather regimes in the surface

impact of sudden stratospheric warming events. *Weather Clim. Dynam.*, **1**(2), 373–388

Hersbach, H., and Coauthors, 2020: The ERA5 global reanalysis. *Q. J. R. Meteorol. Soc.*, **146**(730), 1999–2049

Hitchcock, P., and Coauthors, 2022: Stratospheric Nudging And Predictable Surface Impacts (SNAPSI): A Protocol for Investigating the Role of the Stratospheric Polar Vortex in Subseasonal to Seasonal Forecasts. *Geosci. Model Dev. Discuss.* **15**(13), 5073–5092

Huang, J., Tian, W., Gray, L. J., Zhang, J., Li, Y., Luo, J., and Tian, H., 2018: Preconditioning of Arctic Stratospheric polar vortex shift events. *Journal of Climate*, **31**(14), 5417–5436

Huang, B., and Coauthors, 2021: Improvements of the Daily Optimum Interpolation Sea Surface Temperature (DOISST) Version 2.1. *Journal of Climate*, **34**(8), 2923–2939

Karpechko, A. Y., Charlton-Perez, A., Balmaseda, M., Tyrrell, N., and Vitart, F., 2018: Predicting Sudden Stratospheric Warming 2018 and its Climate impacts with a multimodel ensemble. *Geophysical Research Letters*, **45**(24), 13538–13546

Kobayashi, S., and Coauthors, 2015: The JRA-55 Reanalysis: General Specifications and Basic Characteristics, *J. Met. Soc. Jap.*, **93**(1), 5-48

Kodera, K., Mukougawa, H., Maury, P., Ueda, M., and Claud, C., 2016: Absorbing and reflecting sudden stratospheric warming events and their relationship with tropospheric circulation. *Journal of Geophysical Research: Atmospheres*, **121**, 80-94

Koo, M.-S., and Coauthors, 2022: The Global/Regional Integrated Model System (GRIMs): an Update and Seasonal Evaluation, *Asia-Pac. J. Atmos. Sci.*, https://doi.org/10.1007/s13143-022-00297-y

Martineau, P., Son, S.-W., Taguchi, M., and Butler, A. H., 2018: A comparison of the momentum budget in reanalysis datasets during sudden stratospheric warming events. *Atmos. Chem. Phys.*, **18**(10), 7169-7187

Mitchell, D. M., Gray, L. J., Anstey, J., Baldwin, M. P., and Charlton-Perez, A. J., 2013: The influence of Stratospheric vortex displacements and splits on surface climate. *Journal of Climate*, **26**(8), 2668-2682

Nakagawa, K. I., and Yamazaki, K., 2006: What kind of stratospheric sudden warming propagates to the troposphere? *Geophysical Research Letters: Atmospheric Science*, **33**(4)

Rao, J., Ren, R., Chen, H., Yu, Y., and Zhou, Y., 2018: The Stratospheric Sudden Warming event in February 2018 and its prediction by a climate system model. *Journal of Geophysical Research: Atmospheres*, **123**(23), 13332–13345

Rao, J., Ren, R., Chen, H., Liu, X., Yu, Y., Hu, J., and Zhou, Y., 2019: Predictability of stratospheric sudden warmings in the Beijing Climate Center Forecast System with statistical error corrections. *Journal of Geophysical Research: Atmospheres*, **124**(15), 8385–8400

Rao, J., Garfinkel, C. I., and White, I. P., 2020: Predicting the downward and surface influence of the February 2018 and January 2019 sudden stratospheric warming events in subseasonal to seasonal (S2S) models. *Journal of Geophysical Research: Atmospheres*, **125**(2), 2019JD031919

Seviour, W. J. M., Mitchell, D. M., and Gray, L. J., 2013: A practical method to identify displaced and split stratospheric polar vortex events. *Geophysical Research Letters*, **40**(19), 528–

5273

Sigmond, M., Scinocca, J. F., Kharin, V. V., and Shepherd, T. G., 2013: Enhanced seasonal forecast skill following stratospheric sudden warmings. *Nature Geoscience*, **6**(2), 98-102

Smy, L. A., and Scott, R. K., 2009: The influence of stratospheric potential vorticity on baroclinic instability. *Quarterly Journal of the Royal Meteorological Society*, **135**(644), 1673-1683

Song, K., Son, Seok-Woo, and Woo, Sung-Ho, 2015: Impact of Sudden Stratospheric Warmings on the Surface Air Temperature in East Asia. *Atmosphere*, **25**(3), 461-472

Thompson, D. W. J., Furtado, J. C., and Shepherd, T. G., 2006: On the tropospheric response to anomalous stratospheric wave drag and radiative heating. *Journal of the Atmospheric Sciences*, **63**, 2616-2629

Tripathi, Om P., Charlton-Perez, A., Sigmond, M., and Vitart, F., 2015: Enhanced long-range forecast skill in boreal winter following stratospheric strong vortex conditions. *Environ. Res. Lett.* **10**(10), 104007

White, C. J., and Coauthors, 2017: Potential applications of

subseasonal-to-seasonal (S2S) predictions. *Meteorological Applications*, **24**(3), 315-325

Tables

Table 1. Description of GRIMs model. WRF4 indicates that the relevant physics scheme is adopted from that in WRF model version 4.0. Table from Koo et al. (2022).

	Target	V4.0
Dynamics	Advection	Eulerian + Spectral transform
Physics	Radiation	RRTMG_WRF4
	Surface layer	MO + revision
	Land	Noah V3.4.1_WRF4
	Ocean	Charnock (1955) Taylor et al. (1996)
	Vertical diffusion	YSU_WRF4
	Gravity wave drag by orography	KA_WRF4
	Deep convection	KSAS_WRF4
	Shallow convection	NSCV_WRF4
	Cloud microphysics	WSM3_WRF4
	Cloudiness	Diagnostic_WRF4
Ancillary data	Vegetation fraction	1-km climatology_WRF4
	Maximum snow albedo	Barlage et al. (2005)
	Land use	1-km IGBP-DIS_WRF4
	Soil texture	1-km STATSGO-FAO_WRF4
	CO_2	400 ppmv
	Aerosol	MACC
	Ozone	CAMS

Table 2. Experiments designs for FREE (free-evolving) and NUDGED (stratosphere-nudging) experiments. The nudging method used in this study follows the method of the Stratospheric Nudging and Predictable Surface Impacts (SNAPSI) project and more details in Hitchcock et al. (2022).

		FREE	NUDGED
Configurations	Model	Global/Regional Integrated Model system version 4 (GRIMs V4.0)	
	Resolution	T126 (~1° x 1°) / L64 (0.3 hPa)	
	Initiation date	2018-01-25 00UTC (18 days before the SSW onset)	
	Ensemble	50 ensembles by stochastically perturbed	
Nudging	Reference	No Nudging (Control experiment)	ERA5
	Variables		Zonal mean U & T
	Timescale		six hours
	Domain		Stratosphere (above 90-hPa)

Figures

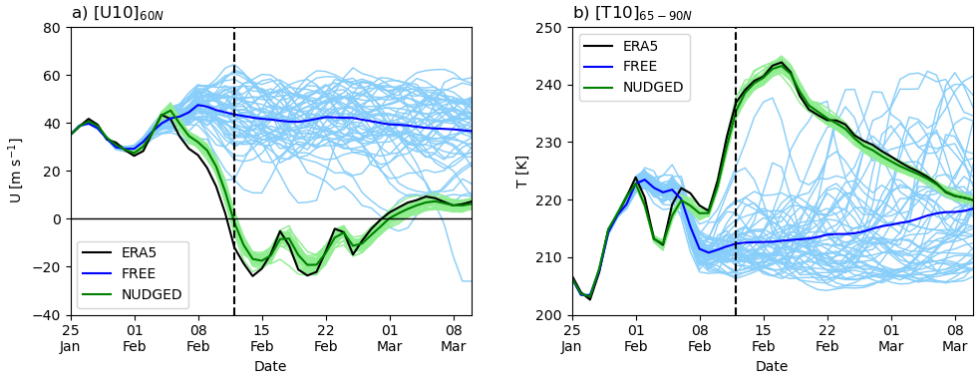

Fig. 1. 10-hPa (a) zonal-mean zonal wind at 60° N and (b) 65-90° N area-averaged temperature for 45 days from 25 January 2018. Black, blue, and solid green lines indicate ERA5, FREE, and NUDGED. Colored solid lines indicate the ensemble mean of each experiment, and colored dashed lines indicate each ensemble. Vertical black dashed lines indicate the onset date of the SSW.

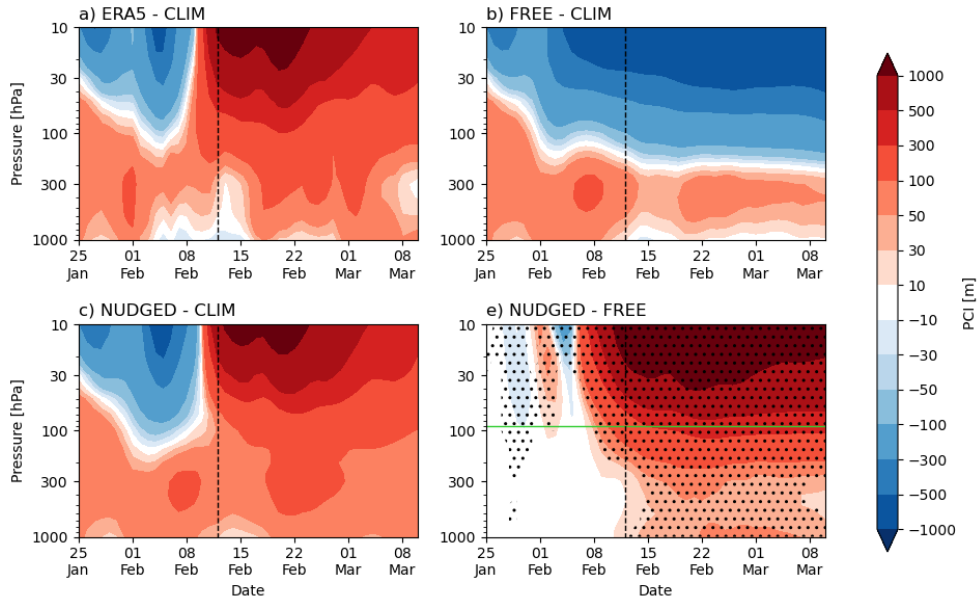

Fig. 2. Time−pressure development of the polar cap (65−90° N) geopotential height anomalies in (a) ERA5, (b)FREE, (c)NUDGED, and (d) the differences between FREE and NUDGED. The dashed black lines indicate the onset date of the SSW, and the green lines indicate the 90−hPa pressure level. Dotted areas indicate statistical significance at the 95% confidence level according to a Student's t−test.

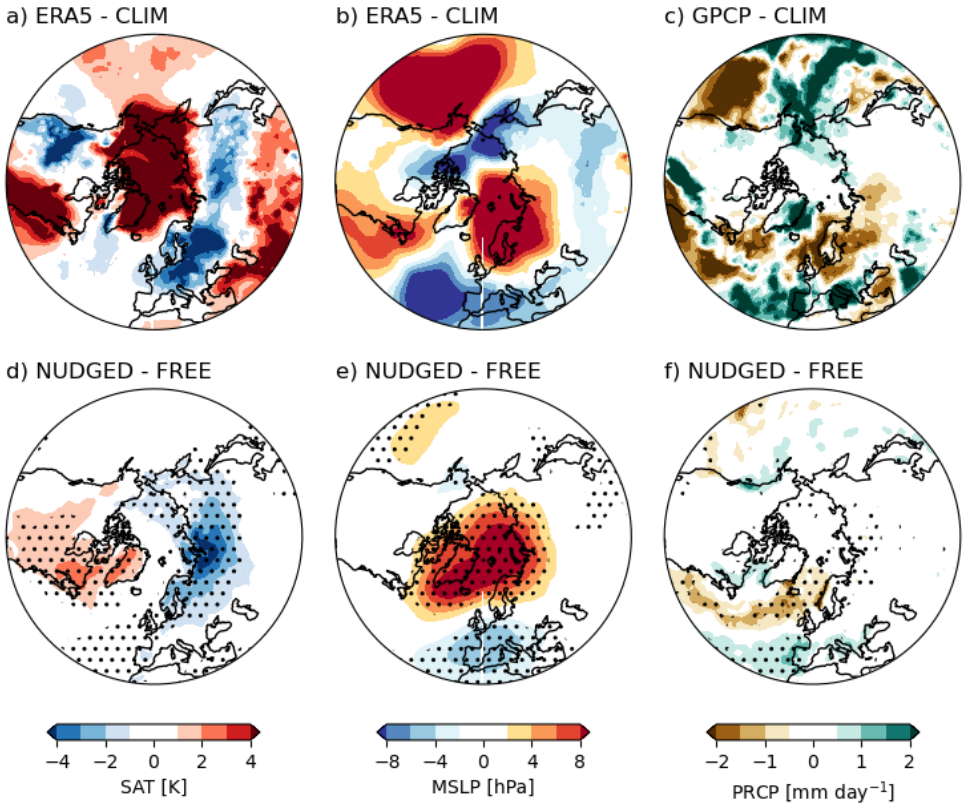

Fig. 3. (a) Surface temperature anomalies. (b) sea−level pressure anomalies and (c) precipitation anomalies in ERA5 and GPCP averaged from 12 February to 3 March. Differences in (d) surface temperature anomalies, (e) sea−level pressure anomalies, and (d) precipitation anomalies averaged over the same period between FREE and NUDGED. Dotted areas indicate statistical significance at the 95% confidence level according to a Student’s t−test.

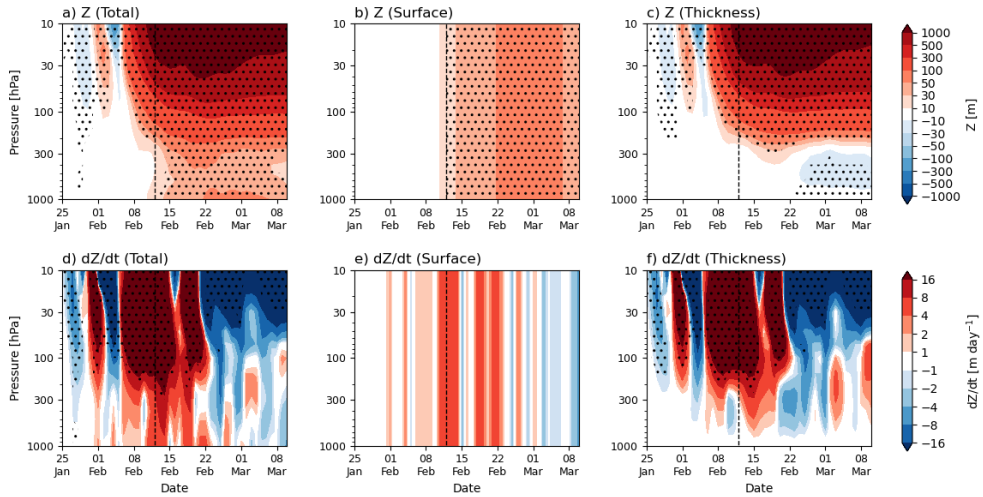

Fig. 4. Time–pressure development of the polar cap (65–90° N) averaged geopotential height differences (NUDGED–FREE) in (a) total, (b) surface, and (c) thickness portions. The same area–averaged differences between geopotential budgets in (d) total, (e) surface, and (f)thickness portions. The dashed black lines indicate the onset date of the SSW. Dotted areas indicate statistical significance at the 95% confidence level according to a Student's t–test.

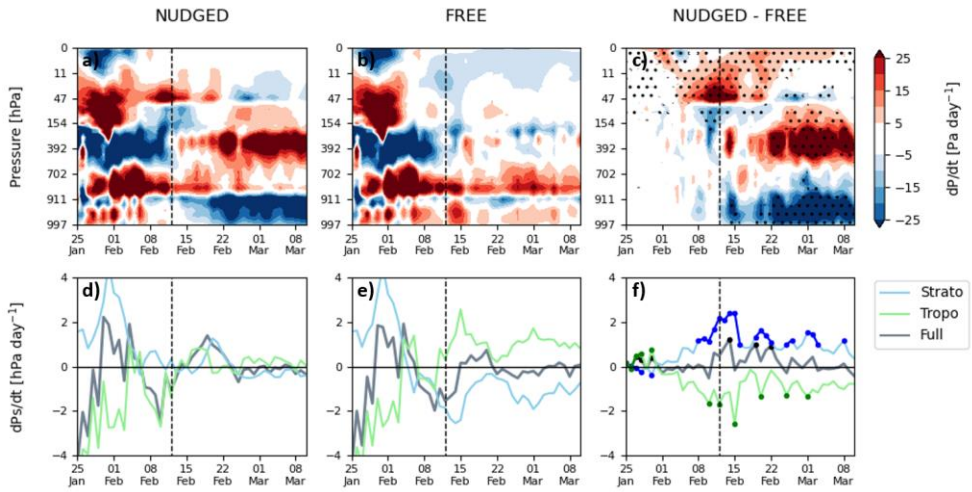

Fig. 5. Time−pressure development of the polar−cap (65−90° N) averaged mass flux convergence(red)/divergence(blue) in (a) NUDGED, (b) FREE, and (c) differences between the two experiments. The evolution of polar−cap averaged surface pressure budgets for each vertical range in (d) NUDGED, (e) FREE, and (f) differences. The dashed black lines indicate the onset date of the SSW. The lower panels' light gray, green, and blue lines indicate the surface pressure budgets from the whole vertical layers, troposphere, and stratosphere. Dotted areas and solid marked lines indicate statistical significance at the 95% confidence level according to a Student's t−test.

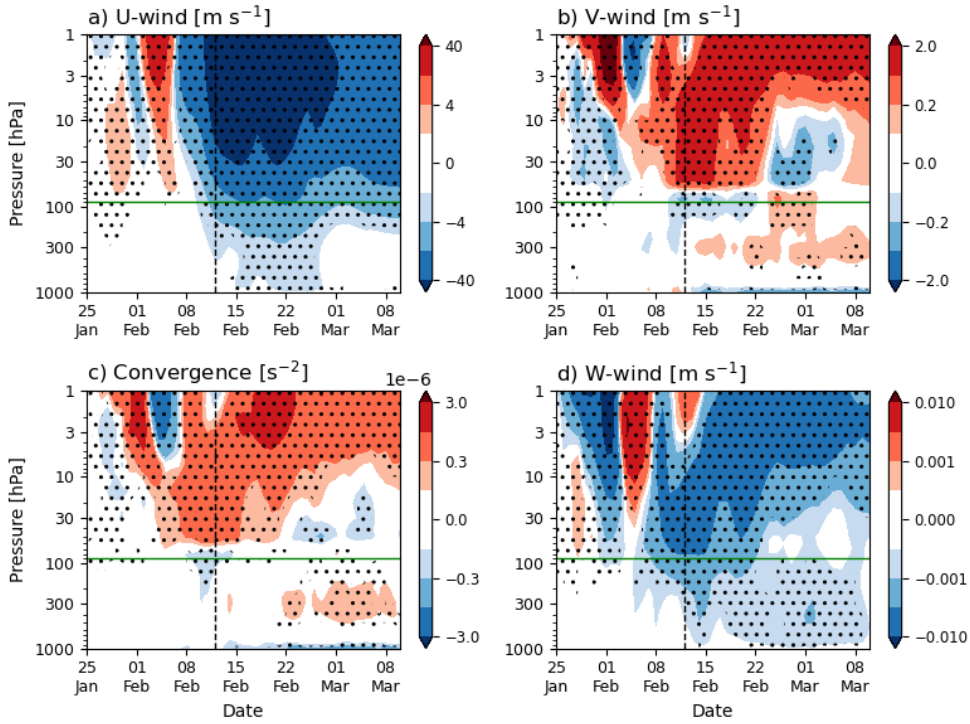

Fig. 6. Time−pressure development of the polar−cap (65−90° N) averaged differences between two experiments (NUDGED−FREE) in (a) zonal wind, (b) meridional wind, (c) convergence, and (d) vertical wind. The dashed black lines indicate the onset date of the SSW, and the green lines indicate the 90−hPa pressure level. Dotted areas indicate statistical significance at the 95% confidence level according to a Student's t−test.

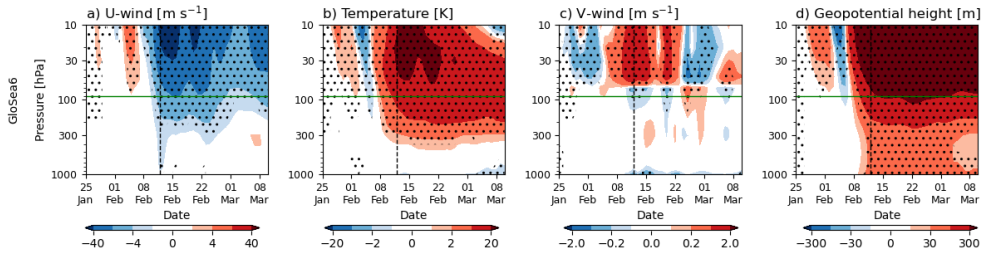

Fig. 7. Time−pressure development of the polar−cap (65−90° N) averaged differences between two experiments (NUDGED−FREE) performed by GloSea6 in (a) zonal wind, (b) air temperature, (c) meridional wind, and (d) geopotential height. The dashed black lines indicate the onset date of the SSW, and the green lines indicate the 90−hPa pressure level. Dotted areas indicate statistical significance at the 95% confidence level according to a Student’s t−test.

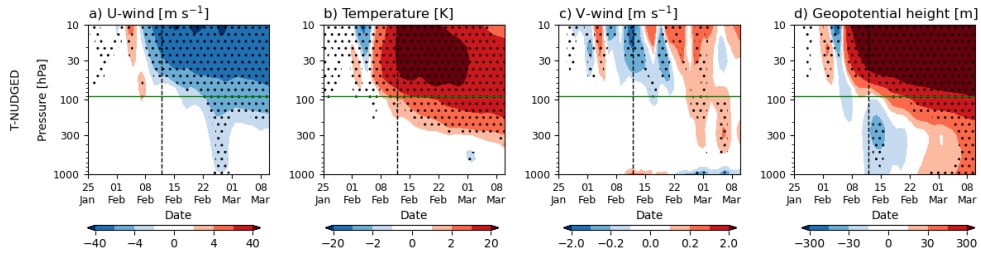

Fig. 8. Same as Fig. 7, but for the differences between FREE and T-NUDGED, only-temperature nudging experiment performed by GRIMs.

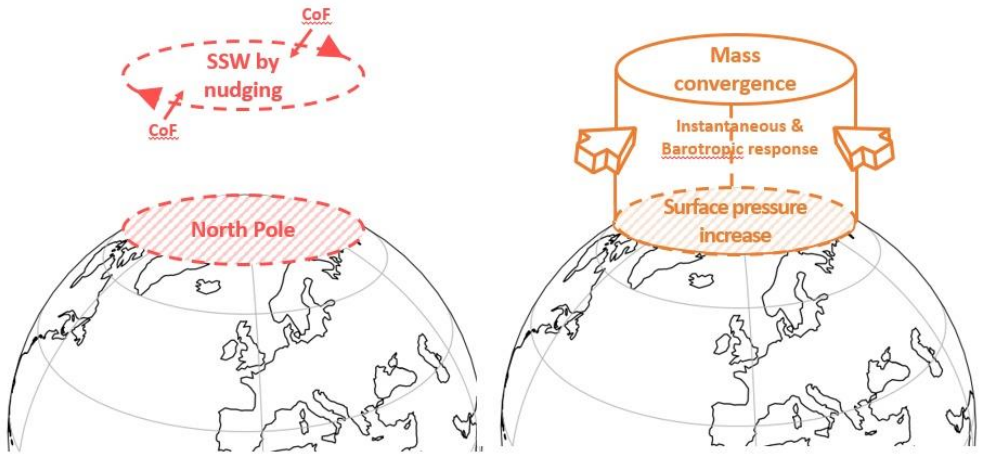

Fig. 9. The schematic diagram of the dynamic process in the SSW nudging experiment.

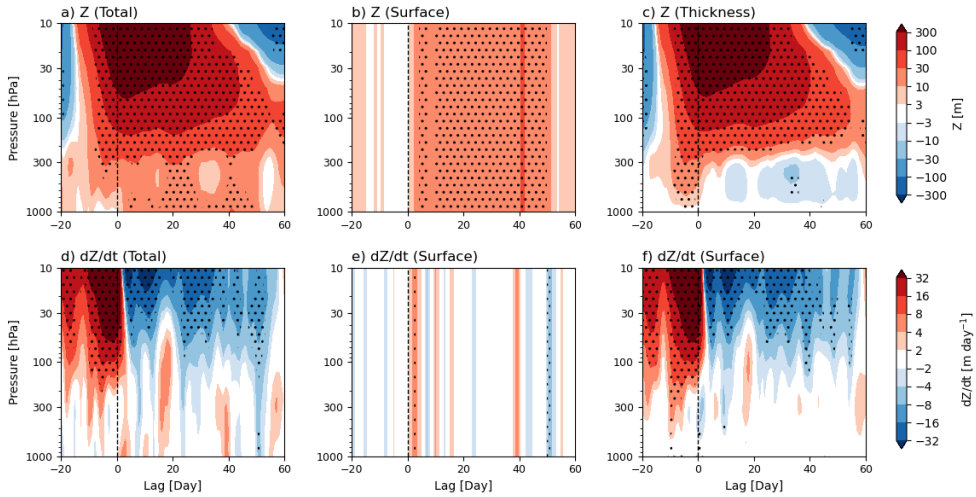

Fig. 10. Same as Fig. 4, but for the polar-cap (65-90° N) averaged geopotential height anomalies during 40 SSWs defined by Charlton and Polvani (2007) in JRA-55.

국문 초록

성층권 동서평균장 너징에 따른 지표 영향: 2018 년 북반구 성층권 돌연승온 사례

홍 동 찬
지구환경과학부
석사과정
서울대학교

2018년 성층권 돌연승온(Sudden Stratospheric Warming; SSW) 현상이 대류권 순환장에 미친 영향을 확인하기 위하여, 전지구 모형인 Global/Regional Integrated Model system (GRIMs)에서 성층권 동서평균 너징 실험이 수행되었다. 너징 없이 수행된 실험(FREE)에서는 발생일 18일 이전에 초기화되면서 돌연승온을 예측하는데 실패하였다. 반면 너징이 진행된 실험(NUDGED)에서는 FREE 실험 대비하여 양의 극지방 지위고도 아노말리(polar-cap geopotential height anomaly index; PCI)와 음의 위상의 북대서양 진동(North Atlantic Oscillation; NAO)을 모의하였다. 2018년 돌연승온의 대류권 영향 메커니즘을 이해하기 위해 지위고도와 표면 기압 버짓 분석이 수행되었다. 두 실험에서 보인 PCI 차이를 지표와 층후 성분으로 나누었을 때, 대류권에서의 PCI 차이는 지표 성분에 의해 나타나며 발생일 부근의 증가가 중요하였음을 지위고도 버짓 분석을 통해 확인하였다. 또한 표면 기압 버짓 분석을 통해 NUDGED 실험의 50-hPa 고도 위에서 강한 공기의 수렴이 존재하였으며, 이

성층권에서의 강한 질량 수렴이 표면 기압을 증가시켰음을 확인하였다. 이러한 성층권 극지방 공기 수렴은 너징으로 인한 동풍 아노말리가 전향력을 받아 극으로 향하는 순환이 발생하면서 나타났으며, Global Seasonal forecasting system (GloSea6) 모형에서의 동일한 실험과 GRIMs 모형에서 온도만 너징하는 두개의 민감도 실험을 통해 민감도를 확인하였다. 본 연구 결과를 통해 성층권의 공기 질량이 적더라도 돌연승온같은 강하고 이례적인 현상은 충분히 표면 기압 변화에 기여할 수 있음을 확인하였으며, 성층권 돌연승온에서 보이는 성층권-대류권 접합과정의 새로운 메커니즘을 제시할 수 있을 것으로 보인다.

주요어: 성층권 돌연승온, 너징, 성층권-대류권 연직 접합, 극지방 지위고도 아노말리, 질량 수렴

학번: 2021-29047